ELSEVIER

Surface Science xxx (2002) xxx–xxx

SURFACE SCIENCE

www.elsevier.com/locate/susc

Correlation of morphology and magnetic properties in ultrathin epitaxial Co films on Au(1 1 1)

N. Spiridis [a], M. Kisielewski [b], A. Maziewski [b], T. Ślęzak [c], P. Cyganik [d], J. Korecki [a,c,*]

[a] *Institute of Catalysis and Surface Chemistry, Polish Academy of Sciences, Kraków, Poland*
[b] *Institute of Experimental Physics, University of Bialystok, Poland*
[c] *Faculty of Physics and Nuclear Techniques, University of Mining and Metallurgy, Al. Mickiewicza 30, 30-59 Kraków, Poland*
[d] *Institute of Physics, Jagiellonian University, Kraków, Poland*

Abstract

Structural and magnetic properties of ultrathin Co films were studied by scanning tunneling microscopy and magneto-optics. Hundred nm Au(1 1 1) films grown epitaxially on mica were used as buffer layers. The initial Co nucleation at the elbows of the "herringbone" reconstruction determined the film morphology, which displayed long chains resulting from the coalescence of the self-organized Co nuclei. A height amplitude of the chains changed considerably upon film annealing. For the ex situ magnetic measurements, wedge samples were prepared, protected with a 5 nm Au layer. Using Kerr magnetometry it was possible to observe the spin reorientation transition. It turned out that the critical thickness decreases for annealed films. The magnetic surface anisotropy was determined and correlated with the film microstructure. © 2002 Published by Elsevier Science B.V.

Keywords: Scanning tunneling microscopy; Epitaxy; Surface structure, morphology, roughness, and topography; Cobalt; Gold; Low index single crystal surfaces; Magnetic films; Metal–metal magnetic thin film structures

1. Introduction

Magnetic films with perpendicular magnetization attract strong attention due to their potential applications for information storage technology [1]. Co ultrathin films grown on Au(1 1 1) belong to the most investigated systems, in which the spin reorientation transition (SRT) takes place [2]. SRT, which means a change of the easy magnetization axis from a perpendicular to an in-plane one, is basically the result of the interplay between interface and shape anisotropy. However, in real systems, anisotropy of thin films is governed by many additional factors resulting from the film microstructure, strains etc. Co films on Au(1 1 1) are especially sensitive to these factors due to their complicated nucleation and growth, determined by the "herringbone" reconstruction of Au [3]. This phenomenon, thoroughly considered and discussed when the growth of self organized cobalt nanostructures is concerned [4], usually is neglected for thicker Co films, close to SRT [5]. It

* Corresponding author. Address: Faculty of Physics and Nuclear Techniques, University of Mining and Metallurgy, Al. Mickiewicza 30, 30-59 Kraków, Poland. Tel.: +4812-617-2911; fax: +4812-634-1247.
E-mail address: korecki@uci.agh.edu.pl (J. Korecki).

0039-6028/02/$ - see front matter © 2002 Published by Elsevier Science B.V.
PII: S0039-6028(02)01307-9

seems, however, that manipulating the interface quality by annealing treatment may lead to severe modifications of the film morphology. For a proper interpretation of the observed effect it is therefore important to combine the characterization of magnetic properties with microscopic measurements of the structure.

After the first observation of the magnetic domain structure [2] a series of in situ works were performed on ultrathin cobalt films deposited on a Au(1 1 1) single crystal, where a huge influence of heat treatment on the magnetic microstructure [5–7] was correlated with a modification of the film morphology. Domains in Co/Au(1 1 1) single crystals were also investigated as a function of the film thickness and carbon content by means of magnetic force microscopy under ultrahigh vacuum conditions [8]. However, complex domain and magnetic anisotropy studies, requiring the proper amplitude and orientation of the magnetic field at the sample, are difficult to perform in situ. For ex situ magnetooptics and domain studies, inexpensive substrates—specially annealed (1 1 1)-textured Au films on glass were used. However, they were not fully comparable with the Au single crystalline substrates [9,10]. In the present study, the microstructure of cobalt films deposited on high quality Au(1 1 1) substrates obtained on mica, was investigated in situ by scanning tunneling microscopy (STM). The correlation of film structure and post-preparation annealing with magnetic anisotropies was studied by means of ex situ magneto-optic measurements on the Au coated Co films.

2. Experimental

Co films were grown on specially prepared Au buffer layers. An epitaxial Au(1 1 1) layer, about 100 nm thick, was grown on mica by thermal evaporation on a heated substrate (600 K). After being flame annealed, the substrate was reintroduced into the UHV system (base pressure 5×10^{-9} Pa) equipped with standard surface facilities (LEED, AES), molecular beam epitaxy (MBE) and a STM head (Aris 1100, Burleigh). After a single crystal like treatment—a few cycles of Ar-ion bombardment/770 K annealing—LEED pattern indicated the (1 1 1)Au surface with the $22 \times \sqrt{3}$ reconstruction. Co films and wedges were evaporated from thermal MBE sources (BeO crucibles) at the rate of about 0.1 nm/min, as calibrated using a quartz balance. The pressure during deposition was kept below 2×10^{-8} Pa.

For ex situ magnetic measurements Co films and wedges were finally covered with a 5 nm Au layer. Room temperature magnetization measurements were performed by the polar Kerr effect using laser light $\lambda = 633$ nm, modulation of light polarization and compensation of the Kerr rotation angle φ. φ fulfills the relation $\varphi = \varphi_{\max}\langle\cos(\theta)\rangle$, where θ is the angle between magnetization and the sample normal. The brackets stand for averaging over the magnetic domain structure. The normal component of mean magnetization can be described by $m = \varphi/\varphi_{\max}$. In a magneto-optical magnetometer, a computer registers the angle φ and controls the magnitudes of both magnetic field components: perpendicular ($H_\perp$) and parallel ($H_\parallel$) to the cobalt film plane. Changes of the angle θ as a function of $H_\perp$ and $H_\parallel$ field magnitudes in a mono-domain state (saturated sample) are described by minimizing the total sample energy, which is given by the following formula:

$$E_{\mathrm{TOT}} = -\mu_0 H_\perp M\cos(\theta) - \mu_0 H_\parallel M\sin(\theta) + K_{1\mathrm{eff}}\sin^2(\theta) + K_2\sin^4(\theta), \quad (1a)$$

where the effective anisotropy constant $K_{1\mathrm{eff}}$ is given by

$$K_{1\mathrm{eff}} = -\mu_0 M_s^2/2 + K_{1\mathrm{v}} + 2K_{1\mathrm{s}}/d. \quad (1b)$$

In the expressions above, the demagnetization term and both the volume and surface anisotropy contributions are taken into account. The angle θ can be calculated for any $H_\perp$ and $H_\parallel$ values minimizing Eqs. (1a) and (1b) if $K_{1\mathrm{eff}}$ and K_2 are known. It is possible to create different surfaces $m(H_\perp, H_\parallel) = \cos[\theta(H_\perp, H_\parallel)]$ for different values of $K_{1\mathrm{eff}}$ and K_2. Thus, both anisotropy constants could be determined by fitting $m(H_\perp, H_\parallel)$ dependencies, measured in a mono-domain state of the sample. A saturation magnetization value $\mu_0 M_s = 1.78$ T of bulk Co was used in the calculations.

3. STM results

The STM images were taken in the topographic mode using electrochemically etched W tips at a typical tip bias 0.8–1.5 V. Examples of the STM images taken on the Au(1 1 1)/mica substrates are presented in Fig. 1. A 1×1 μm^2 scan (Fig. 1a) displays flat terraces separated by single steps or step bunches. The grains (not shown) are typically a few micrometers large. Fig. 2b, chosen at the area with a high step density, shows details of the Au(1 1 1) surface structure. The herringbone reconstruction is clearly visible in the current data. In many features, the reconstruction does not differ substantially from that observed for single crystalline surfaces [11]. The zig-zag structures are however less regular with one section being often much shorter. Moreover, there are areas, where the linear reconstruction is stabilized (indicated by an arrow), as shown previously by Padovani et al. [4]. Terraces separated by single monoatomic steps have an average size of 100 nm and the steps in bunches do not come closer than 7 nm as seen from the section in Fig. 1c.

According to many previous studies [3,4,8,12], Co growth is directly related to the reconstruction of the Au(1 1 1) surface. Co is reported to nucleate at the elbows of the herringbone reconstruction, which results in the self-organization in rectangular lattice. Upon increasing the coverage the Co nuclei coalesce and transform into rows spaced at about 13 nm appear. Such row-like structure is also characteristic of the growth of our films, as can be seen from a large scale STM image in Fig. 2 for a 0.8 nm (4 ML) Co film deposited at room temperature and annealed for 15 min at 250 °C. The image is chosen as showing all typical features observed for as-deposited and annealed films. To better visualize the structure of the Co deposit, the corrugations due to the terrace level have been partially subtracted. Three types of Co structures can be identified: (1) long chains (occupying the largest area), which result from the coalescence of the self-organized Co nuclei, (2) randomly distributed and irregularly shaped Co clusters, and (3) long isolated lines and curves, which appear featureless at this magnification but which are in fact dense packed rows of Co clusters decorating bunches of steps. In principle, similar Co structures were observed by Padovani et al. [4] at the

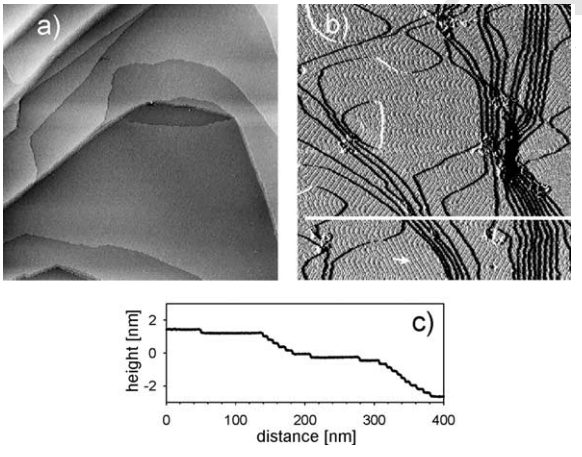

Fig. 1. Au(1 1 1) buffer layer on mica: (a) 1×1 μm^2 STM topographic image of an area with large terraces; (b) 400×400 nm^2 current data visualizing herringbone reconstruction on an area with bunches of monoatomic steps, where the reconstruction is disturbed and (c) section of the corresponding topographic image taken along the marked line.

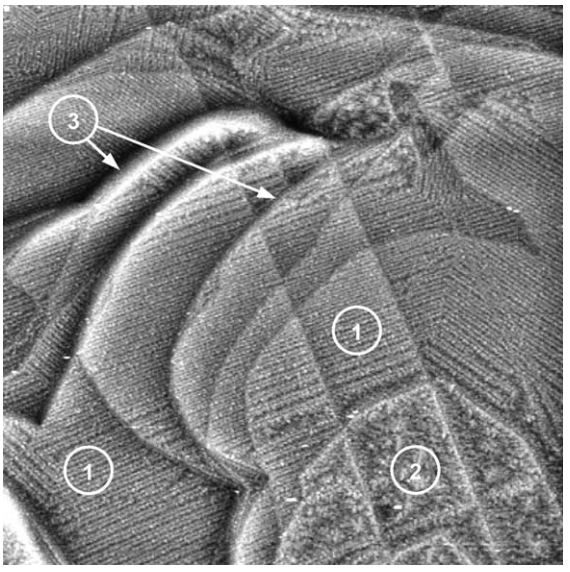

Fig. 2. 1.5×1.5 μm^2 STM topographic image of 4 ML Co deposited on Au(1 1 1)/mica at RT and annealed for 15 min at 520 K. Three types of Co structures, described in the text, are indicated by arrows.

initial growth stage of Co on Au(1 1 1)/mica. An unexpected feature noticed presently is the wealth of chain-like structures that are attributed to Co nucleation sites of the Au reconstruction. We measured at least three different values of the row spacing: 12.6 ± 0.4, 9.8 ± 0.3 and 8.5 ± 0.3 nm, only the first one being in fair agreement with the expected value of 13 nm [11]. Moreover, there is a clear tendency for rows to pair in certain areas and even to gradually change the spacing. In many images of different sizes we checked carefully that the effects described above are not artifacts connected with the scan instability or drifts. Apparently, the cobalt rows reproduce irregularities in the Au reconstruction—additional factors determining the cobalt self-organization, like strains or magnetic interaction, cannot be excluded.

More detailed analysis of film morphology at a 4 ML coverage is done comparatively, following the post-preparation annealing treatment. In Fig. 3, 500×500 nm^2 STM images are presented for the Co deposit in (a) the as-prepared state, (b) annealed for 15 min at 520 K (large scan shown in Fig. 2) and (c) annealed for 60 min at 520 K. The 3D-growth that starts with bilayer clusters [4], proceeds at room temperature for 4 ML films. In the as-prepared state, individual Co clusters are still partially separated and their size is determined by the distance of the adjacent reconstruction elbows, which is about 7.5 nm. The rows remain rather isolated, judging from the section along the marked line, which indicates that the rows have an average height of at least 1.2 nm (6 ML), and occasionally the height amplitudes up to 2.0 nm (10 ML) are found. A good measure of the film roughness is the RMS height value calculated for a single substrate step within a defined area (we take 100×100 nm^2), which was found to be $RMS_{100} = 0.34$ nm. Annealing affects both the lateral and the vertical size scales of cobalt structures. Generally, a granular structure becomes less pronounced and the number of exposed atomic levels decreases upon annealing. As short annealing as 15 min is able to reduce the surface roughness nearly by a factor of 2 ($RMS_{100} = 0.175$ nm), and after 1 h of annealing ($RMS_{100} = 0.13$ nm) the surface displays only two atomic levels over hundreds of nanometers (as seen from the section in Fig. 3c). Even more apparent are the annealing-induced changes of the lateral structure size. Surface flattening is accompanied by a clear coalescence of row-like structures that form now rows, which double or even quadruple their original width. The dominating size of the lateral structures is increased up to 50 nm.

Annealing also leads to the increase of relative intensity in Au/Co Auger peaks. In view of the observed changes of surface topography, such an increase must be interpreted as arising from the Au surface segregation, in agreement with the con-

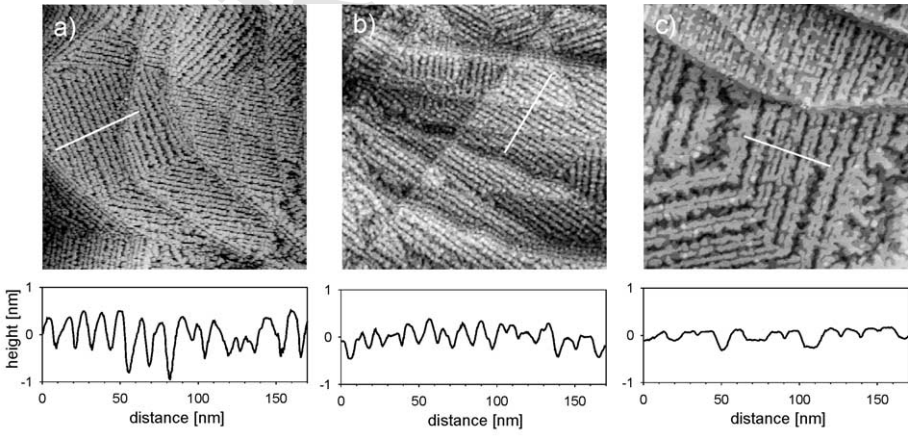

Fig. 3. 500×500 nm^2 STM topographic images of 4 ML Co deposit on Au(1 1 1)/mica: (a) as-prepared at RT; (b) annealed for 15 min at 520 K and (c) annealed for 60 at 520 K. Below, sections along the marked lines are shown.

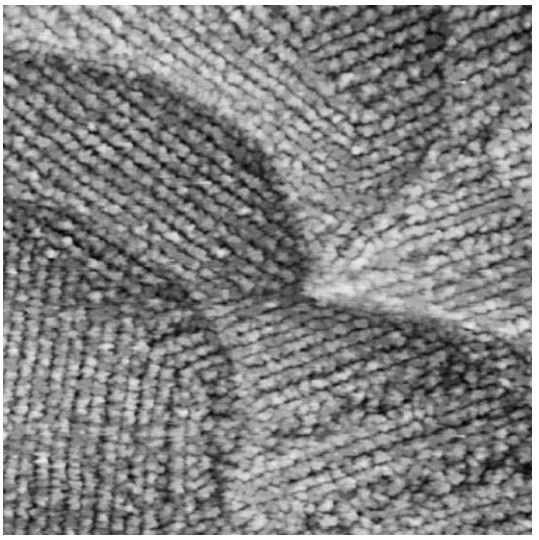

Fig. 4. 500 × 500 nm² STM topographic image of 10 ML Co deposited on Au(1 1 1)/mica at RT, as-prepared.

clusion by Speckmann et al. [5]. At low Co coverage (1.5 ML), Padovani et al. [12] observed annealing-induced incorporation of Co clusters into a Au(1 1 1) substrate, which ends up with complete dissolution into the substrate at 700 K annealing. When discussing the influence of annealing on magnetic properties of non-coated film, one has thus to consider not only a change of the film morphology, but also its covering with gold. It means the interplay of different factors that determine the critical thickness of the spin reorientation transition—film topography and chemical composition of the interface.

The coalescence of the Co films is not completed even at 2 nm (10 ML). The STM image of the as-prepared surface (Fig. 4) reveals similar row-like structures as for thinner films -but the film roughness is considerably reduced (RMS_{100} = 0.145 nm) compared to the non-annealed 4 ML film.

4. Magnetic measurements

Magnetic properties were studied, as described in Section 2, for as-prepared and annealed (60 min at 520 K) films and wedge samples [13]. The magnetic anisotropy for the as-prepared and annealed samples, calculated from Kerr measurements, are shown in Fig. 5a and b, respectively. Because $K_2 > 0$, one can deduce thickness-induced reorientation from an easy axis observed when $d_{Co} < d_1$, through an easy cone ($d_1 < d_{Co} < d_2$) into an easy plane state when $d_{Co} > d_2$. After annealing the reorientation region is shifted towards lower thickness. The opposite (towards greater thickness) annealing induced shift of the reorientation region was in situ observed by Speckmann et al. [2]. Probably, covering of cobalt by gold after annealing is responsible for the shift [2], whereas the effect observed here is purely due to annealing-

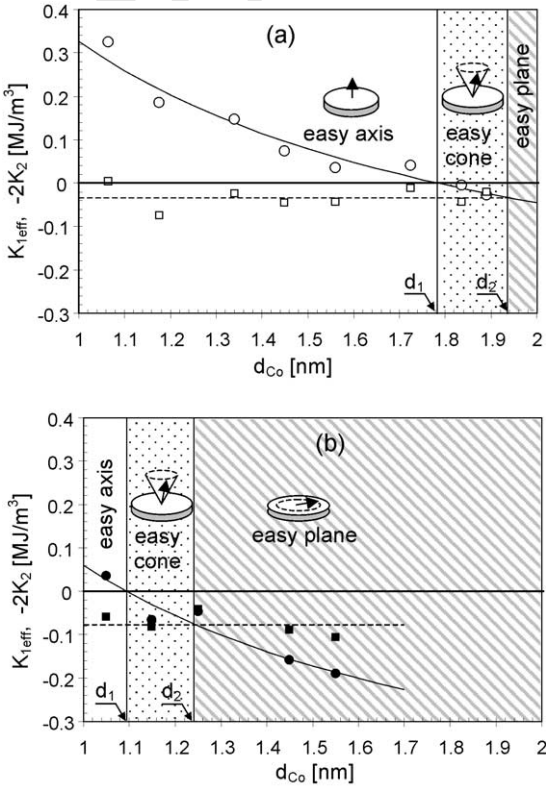

Fig. 5. K_{1eff} (circles) and $-2K_2$ (squares) anisotropy constants as a function of the thickness determined for wedges: (a) deposited at RT (open symbols) and (b) annealed (full symbols) for 60 min at 520 K. Solid curves—fitted K_{1eff} (d_{Co}) dependencies (Eq. (1b)) resulting anisotropy constant values: (a) $K_{1s} = 0.37$ mJ/m² and $K_{1v} = 0.85$ MJ/m³; (b) $K_{1s} = 0.35$ mJ/m² and $K_{1v} = 0.64$ MJ/m³. The dotted lines represent averaged $-2K_2$ values.

induced changes of the film morphology. From the $K_{1\text{eff}}$ versus d_{Co} dependence (Eq. (1b)) the following values of the anisotropy constants have been found: $K_{1s} = 0.37$ mJ/m^2 and $K_{1v} = 0.85$ MJ/m^3 for the as-prepared sample and $K_{1s} = 0.35$ mJ/m^2 and $K_{1v} = 0.64$ MJ/m^3 for the annealed sample. The effective interface anisotropy remains nearly unchanged upon annealing, which only causes changes of the volume-like contribution.

Magnetization reversal was investigated applying a quasistatic magnetic field $H_\perp$ to the films previously saturated by a field much higher than H_c. The dynamics of the process strongly depends on the amplitude $H_\perp$. Let us introduce a demagnetization time, $t_{1/2}$, $(m(t_{1/2}) = 0)$ and a normalized time $t^* = t/t_{1/2}$. For a given film, the character of the magnetization reversal $m(t^*)$ is independent of the magnetic field amplitude (see Fig. 6 for a 0.8 nm Co film). However, one can find the difference of the shape of $m(t^*)$ measured for as-deposited and annealed films. The process undergoes much faster for the as-prepared film. The shape of $m(t^*)$ was described in [14] taking into consideration two mechanisms: *domain nucleation* and *domain wall propagation.* The $m(t^*)$ behavior indicates a bigger contribution of the domain nucleation process in the case of the as-prepared sample. The $t_{1/2}$ versus $H_\perp$ amplitude dependence has an exponential character, as is seen from the inset in Fig. 6. It is possible to estimate the Barkhausen volume V_B assuming that $t_{1/2}$ is proportional to $\exp(-\alpha H_\perp)$ where $\alpha = 2M_s V_B/kT$, k is the Boltzman constant, T is the temperature. By fitting $t_{1/2}(H_\perp)$, the following parameters were obtained: (i) for the as-prepared 0.8 nm film, $V_B = 1700$ nm^3 and lateral volume size $l_B = 46$ nm; (ii) for the annealed 0.8 nm film, $V_B = 5550$ nm^3 and $l_B = 83$ nm. When comparing these results with the Co surface morphology, one can conclude that not a single cobalt island but rather a chain of islands is responsible for the Barkhausen jump.

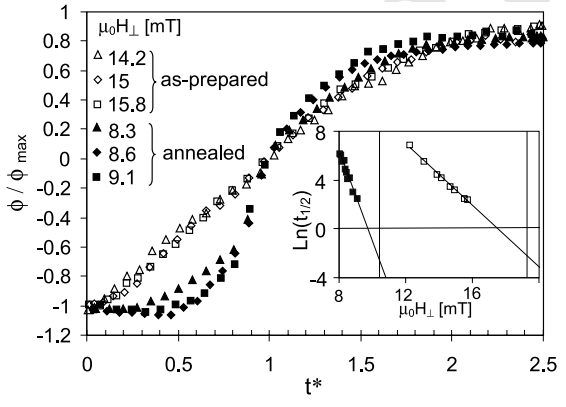

Fig. 6. Magnetization reversal $m(t^*)$ curves registered for different magnetic field $H_\perp$ amplitudes. Insert: dependence of $\ln(t_{1/2})$ on $H_\perp$ amplitude measured for as-deposited (open squares) and annealed (full squares) $d_{Co} = 0.8$ nm films. Vertical lines show coercivity field values measured for both samples.

5. Conclusion

We have found a convincing correlation between the sub-micrometer scale morphology of Co films observed using STM and the magnetic anisotropies measured ex situ by Kerr magnetometry. The most striking result is the annealing-induced decrease of the SRT thickness in contrast with the behavior reported for non-coated Co films [7], which was interpreted as an increase of the effective surface anisotropy induced by annealing. It seems that the presently observed effect is due to the structural and chemical changes of the films contributing to a volume-like anisotropy. Magnetostatic changes: an increase of the demagnetizing energy when the films become smoother, or in other words, change of the roughness anisotropy, could be also involved. Intrinsic Au/Co interface anisotropy remains unchanged. The annealing-induced increase of the Barkhausen volume is clearly connected with the STM detected flattening of the cobalt surface.

Acknowledgements

This work was supported by the Polish State Committee for Scientific Research (grant no. 2P03B 065 15) and the European Science Foundation (NANOMAG project).

References

[1] M.T. Johnson, P.J.H. Bloemen, F.J.A. Broeder, J.J. de Vries, Rep. Prog. Phys. 59 (1996) 1409.
[2] R. Allenspach, M. Stampanoni, A. Bischof, Phys. Rev. Lett. 65 (1990) 3344.
[3] B. Voigtländer, G. Meyer, N.M. Amer, Phys. Rev. B 44 (1991) 10354.
[4] S. Padovani, I. Chado, F. Scheurer, J.P. Bucher, Phys. Rev. B 59 (1999) 11887.
[5] M. Speckman, H.P. Oepen, H. Ibach, Phys. Rev. Lett. 75 (1995) 2035.
[6] H. Oepen, M. Speckmann, Y. Millev, J. Kirschner, Phys. Rev. B 55 (1997) 2752.
[7] H.P. Oepen, Y.T. Millev, J. Kirschner, J. Appl. Phys. 81 (1997) 5044.
[8] M. Dreyer, M. Kleiber, A. Wadas, R. Wiesendanger, Phys. Rev. B 59 (6) (1999) 4273.
[9] J. Pommier, P. Meyer, G. Pénissard, J. Ferré, P. Bruno, D. Renard, Phys. Rev. Lett. 65 (1990) 2054.
[10] J. Ferré, V. Grolier, P. Meyer, S. Lemerle, A. Maziewski, E. Stefanowicz, S.V. Tarasenko, V.V. Tarasenko, M. Kisielewski, D. Renard, Phys. Rev. B 55 (1997) 15092.
[11] J.V. Barth, H. Brune, G. Ertl, R.J. Behm, Phys. Rev. B 42 (1990) 9307.
[12] S. Padovani, F. Scheurer, J.P. Bucher, Europhys. Lett. 45 (1999) 327.
[13] M. Kisielewski, Z. Kurant, A. Maziewski, M. Tekielak, N. Spiridis, J. Korecki, submitted for publication.
[14] E. Fatuzzo, Phys. Rev. 127 (1962) 1999.